



Criterion for the linear convective to absolute instability transition of a jet in crossflow: The countercurrent viscous and round mixing-layer analogy

Davi B. de Souza , Rômulo B. Freitas,^{*} and Leonardo S. de B. Alves [†]

*PGMEC, UFF, Rua Passo da Pátria 156, Bloco E, Sala 211, Niterói,
Rio de Janeiro 24210-240, Brazil*



(Received 17 December 2020; accepted 23 March 2021; published 15 April 2021)

The jet in crossflow, or a transverse jet, eventually undergoes a linear transition from convectively to absolutely/globally unstable as the crossflow to jet velocity ratio increases. This flow field, however, has an extremely complex dynamics. Hence, determining this transition location is not a trivial task. It has long been known that this transition is associated with the upstream shear layer connected to the near field Kelvin-Helmholtz vortex ring, but it was only recently that the most unstable global mode and wave maker were located there as well. These findings led to the realization that an inviscid and planar linear stability analysis of the local velocity profile extracted from the jet in the crossflow upstream shear layer was strongly correlated with its transition to absolute/global instability. It is shown in this paper that such an analysis can be turned into an accurate predictive tool with the use of a viscous (instead of inviscid) and round (instead of planar) mixing layer. In other words, replacing an inviscid analysis of a planar mixing layer with counterflow by a viscous analysis of a round coaxial jet with outer nozzle suction leads to an accurate prediction of the jet in crossflow convective to an absolute instability transition.

DOI: [10.1103/PhysRevFluids.6.L041901](https://doi.org/10.1103/PhysRevFluids.6.L041901)

I. INTRODUCTION

The jet in crossflow, also known as a transverse jet, is formed when a round jet issues perpendicularly into a crossflow. Several vortical structures are generated by the interaction between jet and crossflow in the resulting three-dimensional flow field, such as the counter-rotating vortex pair and the wake vortices in the far field as well as the horseshoe and shear-layer vortices in the near field. This flow has been extensively studied for many decades due to its usefulness in a wide range of technological applications [1]. The reader is referred to the recent reviews in Refs. [2] and [3] for additional information.

Defining appropriate control strategies for this flow field requires knowledge of its linear instability, where concepts such as local (convective/absolute) and global instabilities become relevant [4]. In the absence of crossflow, the transverse jet reverts back to a free jet, which is a well-known convectively unstable flow [5]. Linear stability analysis reveals that this picture does not change in the presence of a weak crossflow, i.e., as long as the crossflow to jet velocity ratio is small enough [6,7]. Hence, free and weak transverse jets are noise amplifiers, which can be controlled with low-amplitude excitation. There is extensive experimental evidence, however, indicating that the transverse jet becomes absolutely/globally unstable when the crossflow gets stronger, i.e., when the crossflow to jet velocity ratio becomes large enough [8–11]. Furthermore, this transition has been confirmed by several different global linear stability analyses [12–14], which associated it with a Kelvin-Helmholtz-type instability of the (upstream) shear-layer that leads to vortex rings. Hence,

^{*} Also at CEFET/RJ, Estrada de Adrianópolis, 1.317, Santa Rita, Nova Iguaçu, RJ 26041-271, Brazil.

[†] lsbalves@id.uff.br

strong transverse jets behave as self-excited oscillators, and their control requires more advanced strategies.

It should be noted that the above studies considered both equidensity and variable density transverse jets as well as transverse jets issuing from either pipes or convergent nozzles that were either flush mounted or elevated. Nevertheless, despite the ubiquitous nature of this transition from convective to absolute/global instability, the critical velocity (or momentum flux) ratio separating both unstable regimes is not the same among these studies. This indicates that even identifying the correct parameter to use in a transition criterion is not a trivial task. Recently, a path towards such a criterion was revealed using data from direct numerical simulations under equidensity and flush-mounted convergent nozzle conditions for $R = 2$ and 4 [15], where $R = U_j/U_\infty$, U_j is the maximum jet velocity and U_∞ is the maximum crossflow velocity. It should be noted that the data are in good qualitative and quantitative agreement with experiments [8]. The criterion proposed was based on the amount of counterflow required to induce a transition to absolute instability in an inviscid and planar mixing layer, quantified though the velocity ratio $R_1 = (V_1 - V_2)/(V_1 + V_2)$. Its critical value, i.e., $R_{1,c} \simeq 1.32$, is well known from classical linear stability analysis [16] and experiments [17]. When applied to the transverse jet, V_1 and V_2 represent the limiting velocities on each side of the profile measured across the upstream shear layer [15, Fig. 21]. This analysis yields $R_1 = 1.44$ and 1.20 for $R = 2$ and 4, respectively, which is consistent with the fact that the transverse jet is absolutely/globally unstable in the former case ($R_1 > R_{1,c}$) and convectively unstable in the latter case ($R_1 < R_{1,c}$). The correlation between both transitions to absolute instability, namely, that of the inviscid and planar mixing layer and that of the jet in crossflow, was clarified in subsequent studies. They showed that the most unstable global mode [14] and the wavemaker [18] are located at the jet in crossflow upstream shear layer when $R = 2$. This is the likely reason why the appearance of counterflow in its local velocity profile due to a stronger crossflow is assumed responsible for this transition. Recent experimental evidence confirmed the relevance of this inviscid and planar mixing-layer analogy [19]. However, it also revealed accuracy issues with this analogy, since it indicates that $R_{1,c} \simeq 1.24$ instead.

Two major assumptions implicit to the inviscid and planar mixing-layer analogy allow the critical velocity ratios obtained from its linear stability analysis [16] and free round jet experiments [17], respectively, $R_{1,c} \simeq 1.315$ and 1.32, to agree so well. The first one is that θ , which is the ratio between mixing-layer thickness and jet diameter, is small enough [20]. This is what allows one to use a planar mixing layer instead of a round jet as the base flow for a linear stability analysis [16] and obtain a result that agrees well with round jet experiments where $\theta \simeq 0.01$ [17]. The second assumption is that Re , which is the Reynolds number based on the jet diameter and maximum velocity, is large enough [21]. This is what allows one to use the Rayleigh equation instead of the Orr-Sommerfeld equation in the linear stability analysis [16] and obtain a result that agrees well with round jet experiments where $Re = 34\,000$ [17]. However, the transverse jet simulations [15] and experiments [19] used in the development of this analogy were performed with $2000 \lesssim Re \lesssim 3000$ and $0.031 \lesssim \theta \lesssim 0.044$. Hence, the inviscid and planar hypotheses are likely inaccurate. This is the reason why a viscous and round mixing-layer analogy should be more appropriate than the originally employed inviscid and planar mixing-layer analogy under these parametric conditions.

In the present paper, the inviscid and planar mixing-layer analogy is extended to a viscous and round mixing-layer analogy through the inclusion of viscosity and the use of cylindrical coordinates in the local, linear, and modal disturbance governing equations. We show that this improvement leads to the development of an accurate predictive criterion based on the critical velocity ratio for the onset of absolute instability of equidensity jets in crossflow. In order to do so, the momentum thickness and Reynolds number effects on the critical velocity ratio required for the transition to absolute instability in coaxial jets must be evaluated.

II. PROBLEM FORMULATION

Both effects can be modeled by the dimensionless continuity and incompressible Navier-Stokes equations written in cylindrical coordinates, where $\vec{u} = \{u, v, w\}$ is the velocity vector, t is time, p is pressure, ν is the dynamic viscosity, and $\text{Re} = U_j D_j / \nu$ is the Reynolds number. This equation was written in dimensionless form using D_j and D_j / U_j as the length and time scales, where D_j is the jet exit diameter and U_j is the maximum jet velocity.

Since the planar mixing-layer analogy uses the classical hyperbolic tangent profile as base flow [16], its well-known extension to a round jet [22]

$$u_b^* = \frac{V_1 + V_2}{2} - \frac{V_1 - V_2}{2} \tanh \left[\frac{1}{8\theta} \left(2r - \frac{1}{2r} \right) \right] \quad \text{and} \quad v_b^* = w_b^* = 0, \quad (1)$$

which satisfies the shear layer momentum thickness definition

$$\theta = \int_0^\infty \left(\frac{u_b^* - V_2}{V_1 - V_2} \right) \left(1 - \frac{u_b^* - V_2}{V_1 - V_2} \right) dr, \quad (2)$$

is employed here, where the superscript $*$ means dimensional and the subscript b means base flow. Although this base flow is assumed local, i.e., its streamwise variation is neglected, the parameters θ , V_1 , and V_2 can assume different values depending on the streamwise location where the profile is measured. The latter two respectively represent the average maximum and minimum velocities on opposite sides of the center plane upstream shear layer [15].

Considering now linear and modal disturbances, one can employ the asymptotic expansion around the above base flow $\mathbf{q}(\mathbf{x}, t) = \mathbf{q}_b(r) + \epsilon \mathbf{q}_n(r) e^{i(\alpha x + m\theta - \omega t)} + O(\epsilon^2) + \text{c.c.}$, where $\mathbf{x} = \{x, r, \theta\}$ is the coordinate vector, $\mathbf{q} = \{u, v, w, p\}$ is the variable vector, ϵ is a small dimensionless parameter associated with the disturbance amplitude, c.c. means complex conjugate, $\mathbf{q}_n(r)$ is the eigenfunction vector, and the eigenvalues are given by the complex stream wise wave number α , the integer azimuthal wave number m , and complex frequency ω . Substituting this decomposition into the continuity and Navier-Stokes equations and collecting the linear terms, i.e., terms of $O(\epsilon)$, leads to the governing equations for the local, linear, and modal disturbances [21] and their respective boundary conditions [23].

Two different methods were used to solve this differential eigenvalue problem, namely, the shooting method and matrix forming. The former was employed to solve the Rayleigh equation for an inviscid round jet [7], obtained in the $\text{Re} \rightarrow \infty$ limit, and an inviscid and planar mixing layer [24], solved here for comparison purposes. It was implemented using the Mathematica [25] built-in functions NDSOLVE and FINDROOT for the initial value problem and search procedure, respectively. Further details can be found elsewhere [7,24]. The latter method was applied to the system of equations, which is a nonlinear differential eigenvalue problem when solving for the stream wise wave number. Hence, it was first rewritten as a linear differential eigenvalue problem using the companion matrix method [26]. A sixth-order central differences scheme was then applied to all spatial derivatives in these equations, transforming them into an algebraic generalized eigenvalue problem. The shift-and-invert Arnoldi method [27] was then employed to generate the Hessenberg matrix, whose Ritz values were calculated with the ZGEEV subroutine from LAPACK [28].

Numerically determining the onset of absolute instability is not trivial when the differential eigenvalue problem cannot be easily reduced to a simple and analytical dispersion relation [29]. Doing so requires locating the relevant saddle/cusp points and proving causality. The original method requires proving the existence of a steepest descent integration path passing through these points. A much simpler alternative is to graphically identify points formed by the collision of downstream and upstream propagating spatial branches, also known as the collision criterion. Both methods simultaneously identify these points and prove causality, but they are computationally time consuming. It is much cheaper to first identify saddle/cusp points and prove causality afterwards. One way to search for these points is to solve the eigenvalue problem coupled with a numerical dispersion relation formed by the discretization of the zero group velocity condition. However,

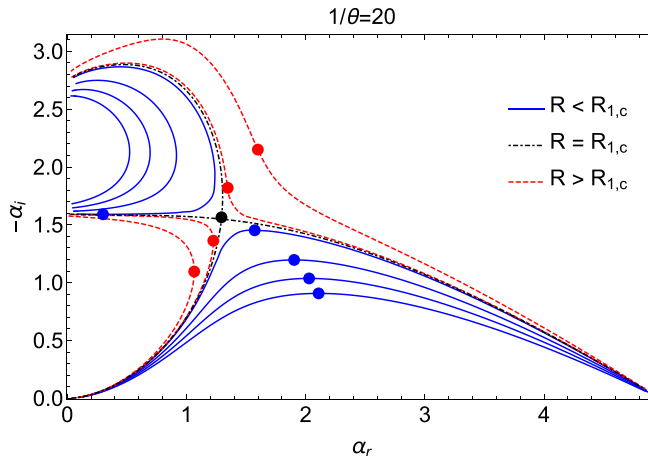


FIG. 1. Collision check for the inviscid ($Re \rightarrow \infty$) axisymmetric ($m = 0$) mode of the round jet with $1/\theta = 20$ at the onset of absolute instability ($R_{1,c} = 1.312374$). Symbols are placed on the steepest ascent (blue) and descent (red) paths passing through the saddle point (black).

convergence can be an issue. Furthermore, the extensions of all three approaches to three-dimensional problems are, essentially, unfeasible. In order to circumvent these issues, an alternative was recently proposed which allows the derivation of auxiliary differential eigenvalue problems. They allow the fast identification of these points when coupled with the original differential eigenvalue problem, even for three-dimensional problems [24]. This approach was employed here.

III. RESULTS

A. Verification

Before proceeding any further, it is important to verify that these codes yield accurate numerical solutions. In order to do so, the streamwise velocity component defined in Eq. (1) is written in dimensionless form using $u_b = (u_b^* - V_2)/(V_1 - V_2)$, and the momentum thickness is assumed to be $\theta = 0.16$. The linear stability results based on the data are then compared with the literature [21, Fig. 8], yielding an excellent agreement.

Finally, the analysis shown next refers to the onset of absolute instability. As mentioned in the previous section, inviscid results for the planar mixing layer and round jet were calculated using a saddle point search procedure based on the shooting method, whereas their viscous counterparts were obtained using the collision criterion based on a matrix-forming procedure. Hence, causality must still be proved for the former and has already been intrinsically demonstrated for the latter. This was done for all the inviscid data points but shown here in Fig. 1 only for the onset of absolute instability of the round jet inviscid axisymmetric mode with $\theta = 0.05$. Symbols are placed on the steepest ascent (blue) and descent (red) paths passing through the saddle point. The former is associated with the wave packet group velocity, whereas the latter demonstrates causality [24].

B. Validation

The importance of viscous effects on the onset of absolute instability in coaxial jets is evaluated first. This is done here by comparing the values of $R_{1,c}$ for the viscous and inviscid round jets, respectively named $R_{1,vis}$ and $R_{1,inv}$. The ratio between these values is shown in Fig. 2 for the axisymmetric, first and second helical modes as a function of the Reynolds number with $D/\theta^* = 12.5$ (left) and 20 (right). Two sets of vertical dashed lines are also shown in this figure, indicating the Reynolds number where $R_{1,vis}$ is 90% and 99% away from its asymptotic value $R_{1,inv}$ for each mode.

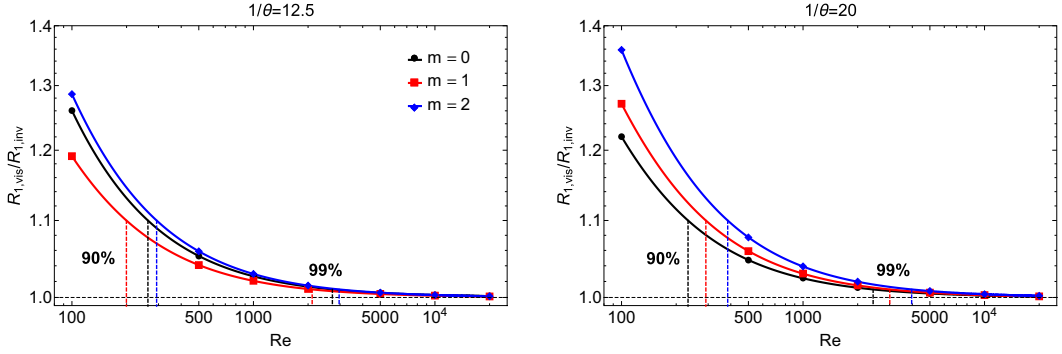


FIG. 2. Ratio between viscous and inviscid round jet velocity ratios at the onset of absolute instability for the axisymmetric, first and second helical modes versus Reynolds number with $D/\theta^* = 12.5$ (left) and 20 (right). Vertical dashed lines indicate the Reynolds numbers where the 90% and 99% difference between viscous and inviscid thresholds occurs for each mode.

These results indicate that viscous effects become negligible, i.e., the 99% threshold is reached, when $2000 \lesssim Re \lesssim 4000$. Hence, they should have a small impact on the ability of the viscous and round mixing-layer analogy to predict the transition to absolute instability observed in recent transverse jet simulations [15] and experiments [19], where $2000 \lesssim Re \lesssim 3000$. Nevertheless, two additional remarks are relevant. First, decreasing the Reynolds number has a stabilizing effect on transition. This means viscous effects will become more relevant if these simulations/experiments are performed at lower Reynolds numbers. Second, increasing the momentum thickness has a stabilizing effect on the axisymmetric mode but a destabilizing effect on both helical modes. This is the reason why transition first occurs for the axisymmetric mode when $D/\theta^* = 20$ but for the first helical mode when $D/\theta^* = 12.5$. Although not shown here, results for $D/\theta^* = 30$ and 20 are qualitatively similar.

The importance of using cylindrical coordinates on the onset of absolute instability in round mixing layers is evaluated next. In order to simplify this analysis, viscous effects are neglected by considering the infinite Reynolds number limit. The impact caused by this cylindrical/Cartesian coordinate choice is then evaluated by comparing the values of $R_{1,c}$ for round jets and planar mixing layers. The ratio between these values, respectively named $R_{1,RJ}$ and $R_{1,PML}$, is shown in Fig. 3 (left)

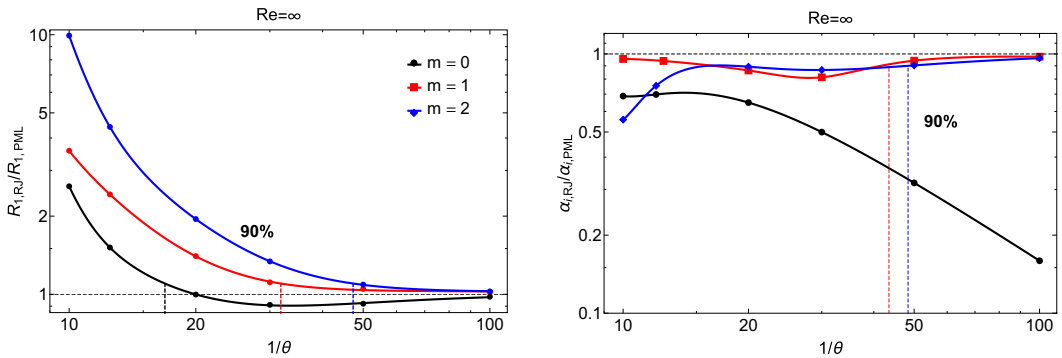


FIG. 3. Ratio between round jet and planar mixing-layer (left) velocity ratio and (right) spatial growth rate at the onset of absolute instability for the axisymmetric, first and second helical modes versus the inverse of the momentum thickness with $Re = \infty$. Vertical dashed lines indicate the momentum thicknesses where the 90% difference between round and planar thresholds occurs for each mode.

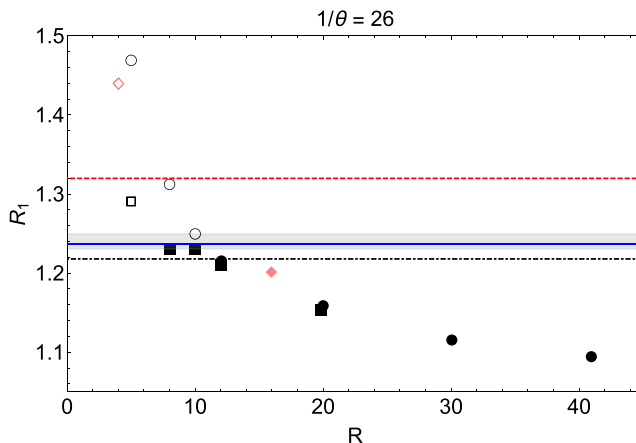


FIG. 4. Experimental data showing R_1 as a function of R . Filled and empty symbols represent data in the convectively and absolutely unstable regions, respectively. Thick horizontal gray band represents $R_{1,c}$ within experimental error [19]. $R_{1,c}$ predictions from the inviscid and planar (red dashed line), inviscid and round (black dot dashed line), as well as viscous and round (blue solid line) mixing-layer analogies for $D/\theta^* = 26$ (at $R \sim 10$) are also shown.

for the axisymmetric, first and second helical modes as a function of the inverse of the momentum thickness. Vertical dashed lines in this figure indicate the momentum thicknesses where $R_{1,RJ}$ is 90% away from its asymptotic value $R_{1,PL}$ for each mode. These results show that the planar hypothesis is inaccurate for the onset of absolute instability prediction within the momentum thickness range observed in recent transverse jet simulations [15] and experiments [19], where $23 \lesssim 1/\theta \lesssim 32$. Furthermore, two important remarks must be made. First, decreasing the momentum thickness has a destabilizing effect on the first and second helical modes. The same is true for the axisymmetric mode, but only up to a certain point. Doing so beyond it has a stabilizing effect instead. Second, this ratio decreases below 1 and approaches its asymptotic limit from below for the axisymmetric mode. Both phenomena are likely linked to the fact that the planar mixinglayer has a single asymmetric mode. Hence, all round jet helical modes must collapse to it, whereas the axisymmetric mode must vanish as $\theta \rightarrow 0$. This is illustrated in Fig. 3 (right), which shows the ratio between round jet and planar mixing-layer spatial growth rates at the onset of absolute instability for the same three modes as a function of the inverse of the momentum thickness. It shows that the spatial growth rate of the axisymmetric mode goes to zero as the momentum thickness is decreased. Although not shown here, the same is true for the wave number and frequency at the onset of absolute instability.

Having clarified the relative importance of viscous effects and cylindrical coordinates within the parametric range previously investigated both numerically and experimentally, the accuracy of the viscous and round mixing-layer analogy can now be quantified. Figure 4 shows experimental data available in the literature [19, Fig. 6] for R_1 as a function of R , indicating the regions of convective (filled symbols) and absolute (empty symbols) instability. The thick horizontal gray band shows the transition between both regions within experimental error, where $R_{1,c} = 1.24 \pm 0.013$. This figure also includes predictions from the analogies discussed here. The values of V_1 , V_2 , and θ were taken from the literature [19, Figs. 5 and 7]. As already discussed in the introduction, the inviscid and planar mixing-layer analogy (red dashed line) yields $R_{1,c} \simeq 1.32$, which has a relative error of 6.42%. The use of cylindrical coordinates, i.e., an inviscid and round mixing-layer analogy (black dot dashed line), improves this result to $R_{1,c} \simeq 1.218$. This means the relative error is reduced to 1.79%. Adding viscous effects, i.e., a viscous and round mixing-layer analogy (blue solid line), further improves this result to $R_{1,c} \simeq 1.237$. In other words, the relative error is further reduced to 0.236% and is now within the experimental error.

IV. CONCLUSIONS

Recently the transverse jet velocity profile measured at its upstream shear layer, where the dominant global mode [14] and wavemaker [18] are located, was employed in an inviscid and planar stability analysis [15]. The authors were able to show that this analysis, i.e., an inviscid and planar mixing-layer analogy, was correlated with the convective/absolute instability nature of the transverse jet.

In the present paper, however, it was noted that the Reynolds numbers and the (inverse of the) momentum thicknesses used in these simulations [15], as well as the experiments they attempted to reproduce [8], were not high enough for the respective inviscid and planar assumptions to be sufficiently accurate. This issue was then overcome by including viscous effects and using cylindrical coordinates in our analysis, effectively creating a viscous and round mixing-layer analogy. Comparisons with experimental data [19] showed that doing so led to the creation of an accurate criterion for the transition to absolute/global stability in transverse jets. Furthermore, the use of cylindrical coordinates was more important than the inclusion of viscous effects for the parametric conditions explored. Nevertheless, the present study also showed how the relative importance of each effect can be estimated *a priori*.

Future work on this topic includes the application of the viscous and round mixing-layer analogy to transverse jets operating under different conditions, such as issuing from elevated convergence nozzles, flushed and elevated pipes, and so on. Furthermore, this analogy is also being extended to predict the onset of absolute instability in variable density transverse jets. This extension is not trivial due to the extreme sensitivity of the stability results to the density profile [30]. Additional experiments are currently being performed by the same UCLA group [19] to evaluate the robustness of this analogy to all these conditions.

ACKNOWLEDGMENTS

The authors would like to express their gratitude to Elijah Harris and Ann Karagozian from the MAE Department at UCLA for their support with the transverse jet experimental data. Davi Souza would also like to thank Ann Karagozian and her research group for welcoming him for one year at UCLA as well as CAPES for the doctorate fellowship.

-
- [1] A. R. Karagozian, Transverse jets and their control, *Prog. Energy Combust. Sci.* **36**, 531 (2010).
 - [2] K. Mahesh, The interaction of jets with crossflow, *Annu. Rev. Fluid Mech.* **45**, 379 (2013).
 - [3] A. R. Karagozian, The jet in crossflow, *Phys. Fluids* **26**, 101303 (2014).
 - [4] P. Huerre and P. A. Monkewitz, Local and global instabilities in spatially developing flows, *Annu. Rev. Fluid Mech.* **22**, 473 (1990).
 - [5] A. Michalke, Survey on jet instability theory, *Prog. Aerospace Sci.* **21**, 159 (1984).
 - [6] R. E. Kelly and L. S. de B. Alves, A uniformly valid asymptotic solution for the transverse jet and its linear stability analysis, *Philos. Trans. R. Soc. London A* **366**, 2729 (2008).
 - [7] L. S. de B. Alves, R. E. Kelly, and A. R. Karagozian, Transverse jet shear layer instabilities. Part II: Linear analysis for large jet-to-crossflow velocity ratios, *J. Fluid Mech.* **602**, 383 (2008).
 - [8] S. Megerian, J. Davitian, L. S. de B. Alves, and A. R. Karagozian, Transverse jet shear layer instabilities. Part I: Experimental studies, *J. Fluid Mech.* **593**, 93 (2007).
 - [9] J. Davitian, D. Getsinger, C. Hendrickson, and A. R. Karagozian, Transition to global instability in transverse jet shear layers, *J. Fluid Mech.* **661**, 294 (2010).
 - [10] D. R. Getsinger, C. Hendrickson, and A. R. Karagozian, Shear layer instabilities in low-density transverse jets, *Exp. Fluids* **53**, 783 (2012).
 - [11] D. R. Getsinger, L. Gevorkyan, O. I. Smith, and A. R. Karagozian, Structural and stability characteristics of jets in crossflow, *J. Fluid Mech.* **760**, 342 (2014).

- [12] S. Bagheri, P. Schlatter, P. J. Schmid, and D. S. Henningson, Global stability of a jet in crossflow, *J. Fluid Mech.* **624**, 33 (2009).
- [13] A. Peplinski, P. Schlatter, and D. Henningson, Global stability and optimal perturbation for a jet in cross flow, *Eur. J. Mech. B* **49**, 438 (2015).
- [14] M. A. Regan and K. Mahesh, Global linear stability analysis of jets in cross flow, *J. Fluid Mech.* **828**, 812 (2017).
- [15] P. S. Iyer and K. Mahesh, A numerical study of shear layer characteristics of low-speed transverse jets, *J. Fluid Mech.* **790**, 275 (2016).
- [16] P. Huerre and P. A. Monkewitz, Absolute and convective instabilities in free shear layers, *J. Fluid Mech.* **159**, 151 (1985).
- [17] P. J. Strykowski and D. L. Niccum, The stability of countercurrent mixing layers in circular jets, *J. Fluid Mech.* **227**, 309 (1991).
- [18] M. A. Reegan and K. Mahesh, Adjoint sensitivity and optimal perturbations of the low-speed jet in cross-flow, *J. Fluid Mech.* **877**, 330 (2019).
- [19] T. Shoji, E. W. Harris, A. Besnard, S. G. Schein, and A. R. Karagozian, On the origins of transverse jet shear layer instability transition, *J. Fluid Mech.* **890** (2020).
- [20] A. Michalke, Instabilität eines kompressiblen runden Freistrahls unter Berücksichtigung des Einflusses der Strahlgrenzschichtdicke, *Z. Flugwiss.* **19**, 319 (1971).
- [21] P. J. Morris, The spatial viscous instability of axisymmetric jets, *J. Fluid Mech.* **77**, 511 (1976).
- [22] A. Michalke and G. Hermann, On the inviscid instability of a circular jet with external flow, *J. Fluid Mech.* **114**, 343 (1982).
- [23] M. Lessen and P. J. Singh, The stability of axisymmetric free shear layers, *J. Fluid Mech.* **60**, 433 (1973).
- [24] L. S. de B. Alves, S. C. Hirata, M. Schuabb, and A. Barletta, Identifying linear absolute instabilities from differential eigenvalue problems using sensitivity analysis, *J. Fluid Mech.* **870**, 941 (2019).
- [25] S. Wolfram, *The Mathematica Book*, 5th ed., Wolfram Media (Cambridge University Press, New York, 2003).
- [26] T. J. Bridges and P. J. Morris, Differential eigenvalue problems in which the parameter appears nonlinearly, *J. Comput. Phys.* **55**, 437 (1984).
- [27] Y. Saad, *Iterative Methods for Sparse Linear Systems*, 2nd ed. (SIAM, Philadelphia, 2003).
- [28] E. Anderson, Z. Bai, C. Bischof, S. Blackford, J. Demmel, J. Dongarra, J. D. Croz, A. Greenbaum, S. Hammerling, A. McKenney, and D. Sorensen, *Lapack User's Guide*, Vol. 3rd (SIAM, Philadelphia, 1999).
- [29] S. A. Suslov, Numerical aspects of searching convective/absolute instability transition, *J. Comput. Phys.* **212**, 188 (2006).
- [30] W. Coenen and A. Sevilla, The structure of the absolutely unstable regions in the near field of low-density jets, *J. Fluid Mech.* **713**, 123 (2012).